Carbohydrate Polymers 108 (2014) 313–320

Contents lists available at ScienceDirect

Carbohydrate Polymers

journal homepage: www.elsevier.com/locate/carbpol

Preparation of the sodium salt of high acyl gellan and characterization of its structure, thermal and rheological behaviors

María M. Murillo-Martínez, Alberto Tecante*

Departamento de Alimentos y Biotecnología, Facultad de Química, Universidad Nacional Autónoma de México, Cd. Universitaria, D.F., 04510 Mexico

ARTICLE INFO

Article history:
Received 14 August 2013
Received in revised form 30 January 2014
Accepted 9 February 2014
Available online 25 February 2014

Keywords:
High acyl gellan
Ionic exchange
FTIR
NMR
DSC
Viscoelasticity

ABSTRACT

This work presents a method to obtain the sodium salt of high acyl gellan (NaHAG) from a commercial preparation, LT-100, by ionic exchange and freeze drying without involving alcohol precipitation to recover the modified macromolecule. NaHAG was characterized by atomic absorption spectrophotometry, attenuated total reflectance Fourier transform infrared spectroscopy, X-ray diffraction and proton nuclear magnetic resonance. In addition, gel viscoelasticity, sol–gel transition temperatures from rheological temperature sweeps and differential scanning calorimetry, of both preparations was examined. Up to 87% of the initial weight of LT-100 was recovered as NaHAG. The sodium ion content in NaHAG was 3.2 times greater than in LT-100 and more than 90% of potassium, calcium and magnesium ions present in the original sample were removed. Transition temperatures of LT-100 were significantly higher than those of NaHAG. However, LT-100 gels were slightly stronger and elastic than NaHAG gels. Characterization data from different analyses suggest that the treatment method makes possible to obtain NaHAG with only slight structure modification with respect to LT-100, and could be advantageously utilized to obtain other monovalent and divalent salt forms of high acyl gellan for use in fundamental studies on its properties in aqueous environment.

1. Introduction

Gellan is an anionic exopolysaccharide produced by the non-pathogenic bacterium *Sphingomonas elodea*. Its primary structure consists of a linear tetrasaccharide backbone of →3)-β-D-Glcp-(1→4)-β-D-GlcpA-(1→4)-β-D-Glcp-(1→4)-α-L-Rhap-(1→ (Jansson, Lindberg, & Sandford, 1983; O'Neil, Selvendran, & Morris, 1983). The native form excreted by the bacteria has an L-glyceryl group (—OOCHO—CH_2OH) linked to the O2 position of →3)-β-D-Glcp and an acetyl group (—OOC—CH_3) linked to the O6 position of the same glucose residue (Kuo, Mort, & Dell, 1986). An L-glyceryl substituent is found every repetitive unit and an acetyl group every two repetitive units as shown in Fig. 1. High acyl gellan (HAG) keeps the same substituent groups present in the native form and when these acyl groups are removed by alkaline treatment, low acyl gellan (LAG) is obtained. In this way, according to the acylation degree gellan is referred to as low acyl gellan (partially deacylated) and high acyl gellan (highly acylated) (Prajapati, Jani, Zala, & Khutliwala, 2013; Sanderson & Clark, 1984). Gel forming and texture development properties of HAG and LAG are relevant in commercial applications. Gelation occurs when hot solutions are cooled and polysaccharide chains existing as random coils turn into double helices which subsequently aggregate creating a three-dimensional network. The opposite phenomenon occurs when gels are heated, leading thus to thermoreversible behavior. Depending on polysaccharide and external cation concentration as well as on the type of counterion, i.e. mono or divalent, thermal hysteresis can be present. When this is so, the gelation temperature is lower than the "melting" temperature. Removal of acyl substituents has a significant effect on the rheological behavior, mechanical properties and physical appearance of the gels; HAG gels are opaque, soft and elastic, while LAG ones are clear, hard and brittle. Polysaccharide concentration and metal ions concentration in solution modify the mechanical and structural properties of the gels (Flores-Huicochea, Rodríguez-Hernández, Espinosa-Solares, & Tecante, 2013; Grasdalen & Smidsrod, 1987; Kang, Veeder, & Kaneko, 1982; Rodríguez-Hernandez, Durand, Garnier, Tecante, & Doublier, 2003; Upstill, Atkins, & Attwool, 1986).

The physicochemical and functional properties of gellan in aqueous solution with or without external mono and divalent ions have been studied and characterized by rheometry, potentiometry, viscometry, polarimetry and differential scanning calorimetry (Mazen, Milas, & Rinaudo, 1999; Milas, Shi, & Rinaudo, 1990; Miyoshi, Takaya, & Nishinari, 1996; Morris, Nishinari, & Rinaudo,

* Corresponding author. Tel.: +52 55 56225307; fax: +52 55 56225309.
E-mail address: tecante@unam.mx (A. Tecante).

http://dx.doi.org/10.1016/j.carbpol.2014.02.056
0144-8617/

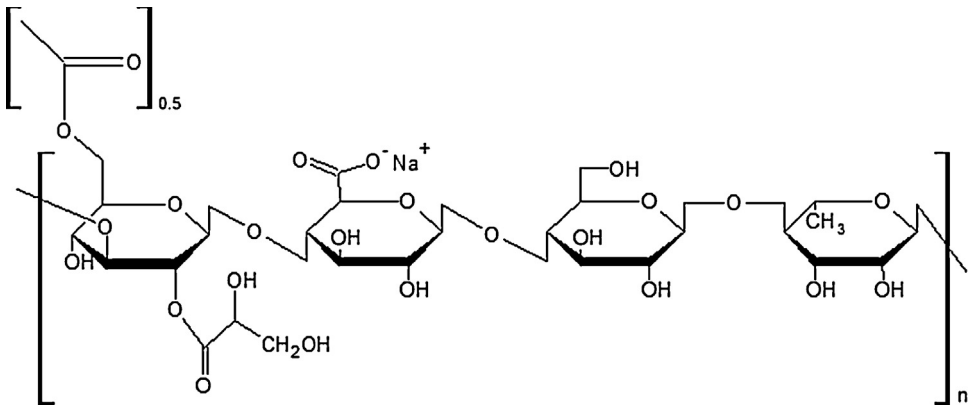

Fig. 1. Ideal structure of the repetitive unit of the sodium salt of high acyl gellan.

2012; Nakamura, Harada, & Tanaka, 1993; Rodríguez-Hernandez et al., 2003). Because of its wide range of rheological, physicochemical and functional properties, gellan has important actual and still potential applications in several fields including food, pharmaceutical, cosmetic and medical. Gellan has become an important choice to generate new, versatile and environmentally friendly materials.

Chemical synthesis and ionic exchange have been applied to modify gellan. Several reaction paths have been explored to replace functional groups in the original gellan backbone, and modification by ionic exchange and recuperation of the modified gellan by precipitation with polar solvents, e.g. acetone, alcohols, alcohol/water mixtures, have been reported (Coutinho et al., 2010; Doner & Douds, 1995; Doner, 1997; Goh, Haisman, & Singh, 2006; Morris et al., 2012; Novac, Lisa, Barbu, Alhaique, & Popa, 2013; Ogawa, Takahashi, Yajima, & Nishinari, 2005; Ogawa, Takahashi, Yajima, & Nishinari, 2006). Due to its importance as a food additive, information about its structure and physicochemical properties is required to develop new methods that allow structure modifications or specific salt forms for particular applications to be obtained. With this point of view, the aim of the present work was to obtain the sodium salt of high acyl gellan (NaHAG) from a commercial preparation (LT-100) by ionic exchange and subsequent freeze drying without involving recuperation of the modified polysaccharide by alcohol precipitation. NaHAG was characterized in terms of its structure and thermal and rheological behaviors. The results presented here could contribute to set up relatively simple treatment methods to obtain a specific salt form of HAG to be used in fundamental studies on its physicochemical behavior in aqueous solution and could also serve as a guide or starting point to obtain other salt forms of this and other food polysaccharides.

2. Materials and methods

2.1. Materials

Commercial high acyl gellan (LT-100) was provided by CPKelco (San Diego, CA, USA). Amberlite® IR-120 (plus) resin was from Sigma–Aldrich (St. Louis, MO, USA). Hydrochloric acid and sodium chloride were from J.T. Baker (Xalostoc, Edo. de Méx., México). All solutions were prepared in deionized water using analytical grade reagents.

2.2. Preparation of the sodium salt of high acyl gellan (NaHAG)

NaHAG was prepared by the method shown in Fig. 2. Amberlite was conditioned by rinsing it several times with water to eliminate possible impurities. The resin was transformed into its acid form (pH 1.0) using 1 M HCl and then rinsed with water until neutrality. The acid Amberlite was suspended in a NaCl solution by stirring at 200 rpm during 10 min and stored at 4 °C for a week. The salt solution was replaced several times during this period and finally the resin was rinsed with water to eliminate NaCl excess. Salt elimination from the resin was monitored with a 0.1 N silver nitrate aqueous solution. The sodium Amberlite was suspended in a 0.7% LT-100 in a 12:1 (w/w) resin to gellan proportion, respectively, and kept under constant agitation at 80 °C during 1 h. After ionic exchange, the resin was filtered from the aqueous solution. The resulting NaHAG solution was evaporated at 40 °C and 72 mbar in a rotary evaporator (Büchi R-205, Switzerland) and freeze dried (Labconco corporation, Kansas City, MO, USA) to obtain dehydrated NaHAG.

2.3. Characterization

2.3.1. AA spectrophotometry

The ion content was determined in an atomic absorption spectrophotometer (Varian SpectrAA 200 A) with an air acetylene flame and a hollow-cathode lamp at wavelengths of 590, 770, 420, 280 nm for Na^+, K^+, Ca^{2+}, Mg^{2+} ions, respectively.

2.3.2. ATR-FTIR

Spectra of LT-100 and NaHAG were obtained in a Spectrum 400 spectrophotometer with an ATR universal accessory (PerkinElmer Cetus Instruments, USA). Measurements were made in the range of 4000–400 cm^{-1} and 32 scans were made with a 4 cm^{-1} resolution.

2.3.3. X-RD

Samples of LT-100 and NaHAG were analyzed in a Siemens D5000 diffractometer with nickel-filtered Cu Kα radiation (λ = 1.54 Å; 40 kV and 40 mA).

2.3.4. ^1H NMR

All measurements were performed at 45 °C in a Bruker Avance DMX of 500 MHz and high resolution (Bruker BioSpin GmbH, Rheinstetten, Germany) with two frequency channels; detection range spectrometer operating from 31 P to 109 Ag. The samples were dissolved in DMSO-d_6.

2.3.5. Solubility in water

Samples of 1.25 mg of LT-100 or NaHAG were stirred in 10 mL deionized water at 800 rpm for 5 h. The percentage transmittance (%T) of LT-100 and NaHAG solutions before and after filtration through a 0.45 μm membrane (Millipore, USA) was measured at 600 nm in a UV/vis spectrophotometer (Thermo SpectronicGenesys10UV, Thermo Fischer Scientific Inc., Waltham, MA, USA) with

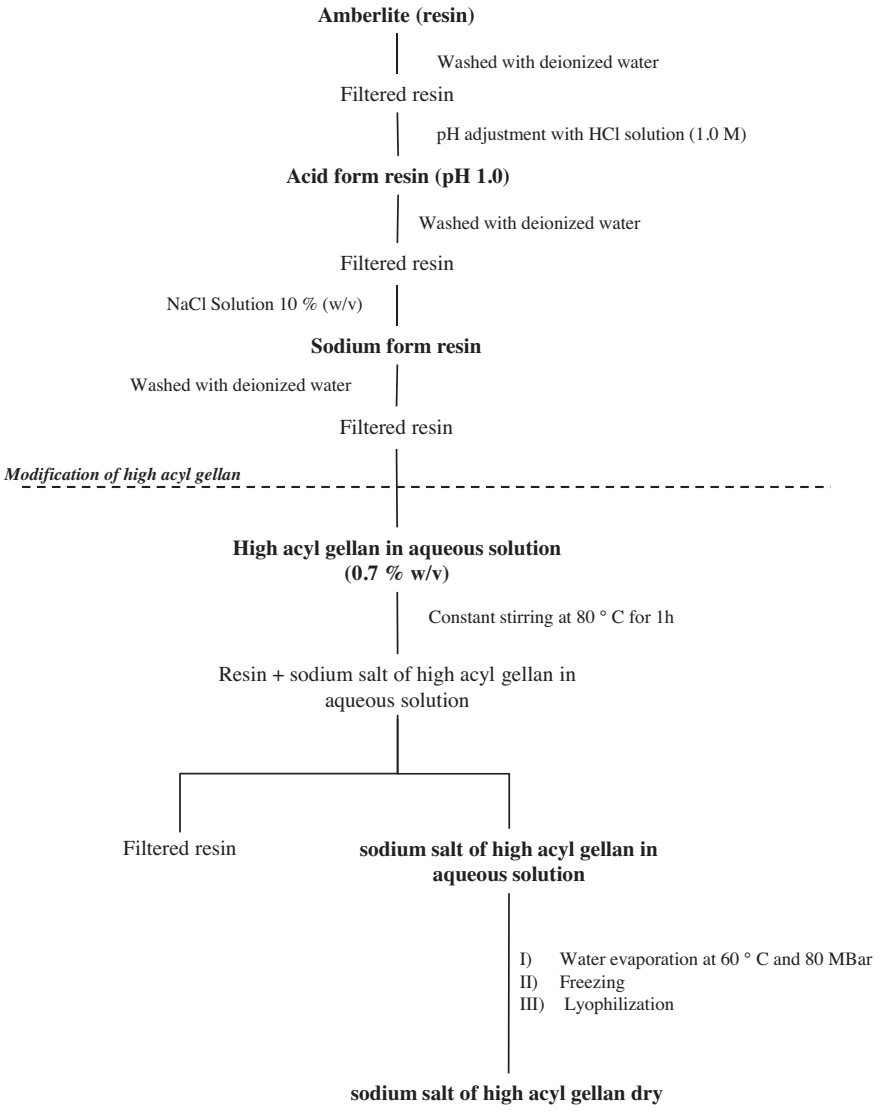

Fig. 2. Preparation of NaHAG from LT-100.

reference to deionized water. The solution with the smallest difference in %T was taken as the one with the highest solubility.

2.3.6. Rheological behavior

Solution preparation and rheological measurements were carried out as described in a previous report (Flores-Huicochea et al., 2013). Aqueous solutions of 1.0% (w/v) of LT-100 and NaHAG were prepared by careful dispersion in deionized water under constant stirring at 300 rpm. Dispersions were heated to 85 °C and stirred at this temperature for 30 min. The evaporated solvent was replaced to maintain the desired polysaccharide concentration. Solutions were degassed for 10 min before testing. The variation of G' and G'' with temperature was examined by means of heating and cooling ramps from 25 to 90 and 90 to 25 °C, respectively, at a heating rate of 1.0 °C/min. Temperature was controlled with a Peltier system. Sol–gel, T_g, and gel–sol, T_m, transition temperatures were determined at the point for $G' = G''$, i.e. $\tan\delta = 1$. Frequency sweeps were run at 25 °C immediately after the cooling temperature sweep. All tests were run in the zone of linear viscoelasticity determined in the range of 0.1–100% strain at an angular frequency of 1.0 Hz (6.28 rad s^{-1}) in an ARES RFS III rheometer (TA Instruments, New Castle, DE, USA) using serrated parallel Plates 25 mm in diameter. The fixture rim was covered with paraffin oil to prevent water evaporation.

2.3.7. Differential scanning calorimetry (DSC)

DSC tests were run in a calorimeter (μDSC 7 Evo, Setaram, France) to determine the thermal behavior of NaHAG and LT-100 in aqueous solution. Samples of 800 mg were placed in standard Hastelloy cells and the reference cell was filled with deionized water. Each sample was tested at a heating rate of 1.0 °C/min with three repeated heating-cooling cycles from 10 to 90 °C and then down to 10 °C, under a nitrogen atmosphere. Sol–gel, T_g, and gel–sol, T_m, temperatures were determined as the peak temperatures from the exo and endothermic transitions, respectively. Onset, T_o, offset, T_f, temperatures and transition enthalpies were also determined.

2.4. Statistical analysis

All statistical analyses were performed using the SPSS version 12.0 software (SPSS Inc., Chicago, IL, USA). The data were tested by an analysis of variance (ANOVA). Comparison of means was performed using Tukey's test. A p value of less than 0.05 was considered statistically significant.

Table 1
Ion content (%) of LT-100 and NaHAG.

Sample	Na^+	K^+	Ca^{2+}	Mg^{2+}
LT-100	0.79	0.45	0.66	0.31
NaHAG	2.55	0.03	0.03	0.016

3. Results and discussion

3.1. NaHAG preparation

The NaHAG obtained was a white and odorless solid. Atomic absorption data (Table 1) shows that 93–95% of the original content of K^+, Ca^{2+} and Mg^{2+} ions was removed from LT-100, while the amount of sodium ion in NaHAG was 3.2 times higher than in LT-100.

3.1.1. ATR-FTIR

Fig. 3 shows ATR-FTIR spectra in the wavelength range of 4000–400 cm^{-1} for LT-100 and NaHAG. LT-100 and NaHAG spectra were similar in shape, but NaHAG exhibited higher transmittance, particularly in the range of 3600–1798 cm^{-1}. The intense bands at 3347.07 cm^{-1} are attributed to OH groups. Vibrations related to C=O, C—O—C and C—O groups appeared approximately at 1737, 1280 and 1028 cm^{-1}, respectively. The signal at 1160 cm^{-1}, corresponds to the glycosidic linkage present in LT-100 and NaHAG. The signal at 1024 cm^{-1} is related to sugars such as mannose, arabinose and rhamnose (Bramhachari & Dubey, 2006; Kačuráková & Wilson, 2001; Sartori, Finch, Ralph, & Gilding, 1997). The spectral bands do not show large changes and modifications that suggest significant alterations in the functional groups for NaHAG obtained from LT-100.

3.1.2. X-RD

Fig. 4 shows the X-ray diffraction spectra for LT-100 and NaHAG. The diffraction pattern of NaHAG has different features not observed for LT-100. The spectrum of LT-100 is characteristic of a mixture of crystalline and amorphous components. Two sharp peaks are observed at $2\theta = 12^\circ$ and 18° with the latter making part of a broad peak at around $2\theta = 20^\circ$ attributed to the presence of the amorphous component. In the diffraction pattern of NaHAG, the sharp peak at about 18° is still observed, but a sharp peak at 30°, not observed for LT-100, appears. The peak at 12°, however, is now less visible than for LT-100. It is apparent from these results that NaHAG and LT-100 have a different organization, giving rise to different diffraction patterns. This change can be attributed to the increase in sodium ions and the decrease in potassium, calcium and magnesium ions. The new peak at 30° can be associated to the presence of larger amounts of Na^+ ion and as a consequence its appearance can be taken as a confirmation of the formation of the sodium salt of high acyl gellan. Although the two samples are predominantly amorphous the decrement in the sharp peaks around 12–25° for LT-100 is attributed to a modification in its crystallinity. The difference in shape of the X-RD patterns suggests a structural modification attributed to the presence of the sodium atoms.

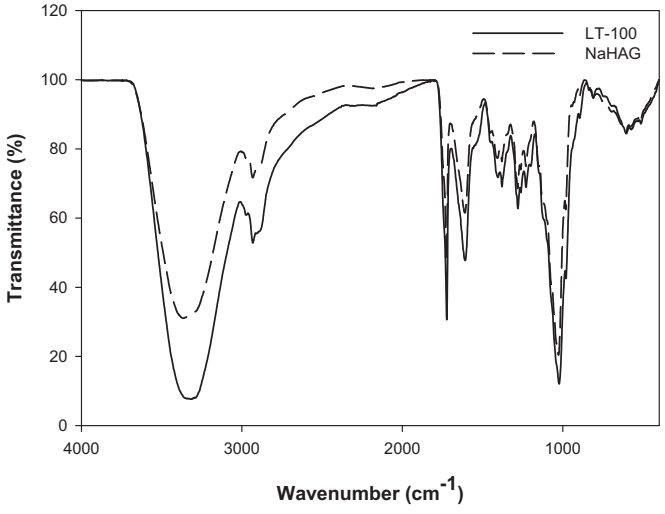

Fig. 3. FTIR-ATR spectra of LT-100 and NaHAG.

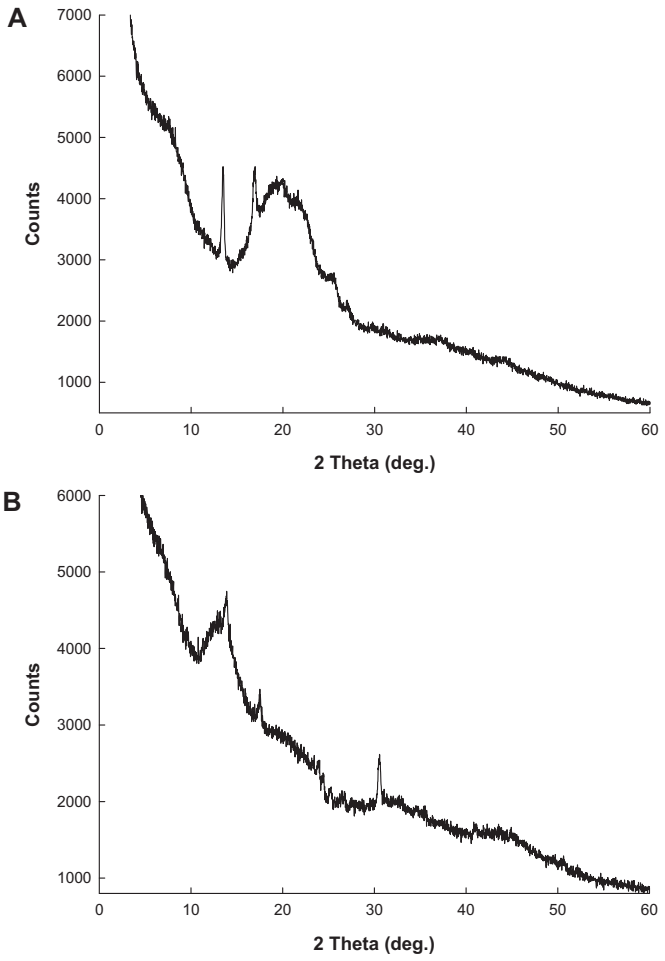

Fig. 4. X-ray diffraction spectra of LT-100 (a) and NaHAG (b).

3.1.3. ^1H NMR

NMR has been used to characterized LAG (Hamcerencu, Desbrieres, Khoukh, Popa, & Riess, 2008; Matsukawa, Tang, & Watanabe, 1999; Milas & Rinaudo, 1996). NMR data for native gellan and HAG are less abundant (Jay et al., 1998; Matsukawa & Watanabe, 2007). For this reason in this work we also examined possible structure modification of NaHAG induced by the ionic exchange treatment. Fig. 5 shows the one-dimensional ^1H NMR spectra for LT-100 and NaHAG. The spectrum for LT-100 was similar to that of NaHAG; clear signals at 2.04 and 1.17 ppm attributed to the protons of the acetate group on (1,3) β-D-glucose (Glcp) and the methyl protons of rhamnose (Rhap), respectively, can be observed (Matsukawa & Watanabe, 2007). In the range of 4.0–5.5 some differences between the spectra for LT-100 and NaHAG were observed. The most interesting changes were in the range of 4.6–5.5; signals around 5.13 and 5.30 ppm are attributed to the anomeric protons (H-1) of Rhap, indicating the existence of a β-D configuration in

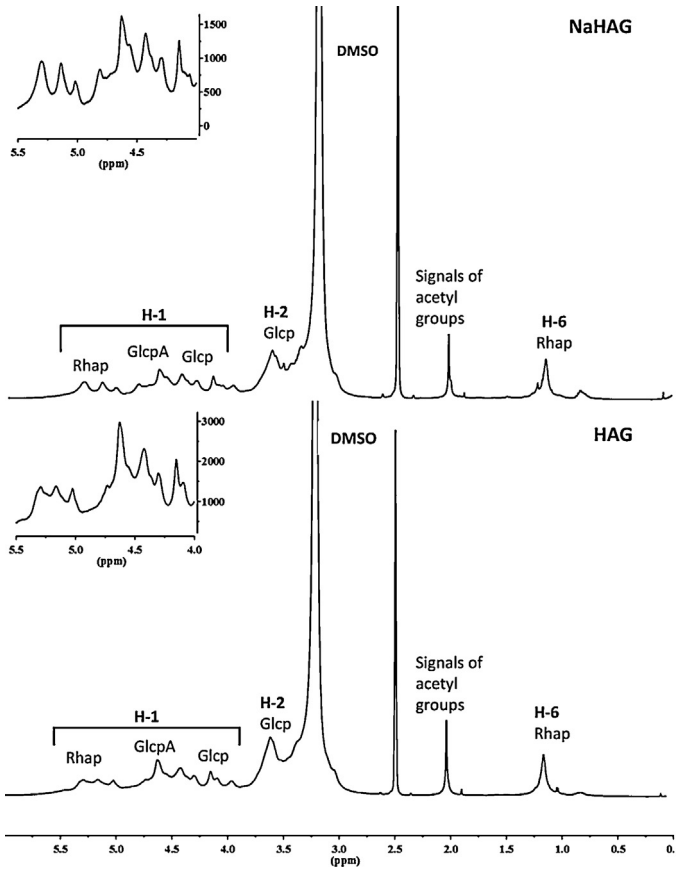

Fig. 5. ^{1}H NMR spectra of LT-100 and NaHAG in DMSO-d_6, at 500 MHz and 318 K.

the polysaccharide chain. The 5.02 ppm signal is assigned to H-1 of Rhap, which suggests an α-L configuration. All these data suggest that the treatment method reported here makes possible to obtain NaHAG with only slight structure modification with respect to LT-100.

3.1.4. Solubility in water

To the best of our knowledge, there are not systematic and quantitative reports on the solubility of gellan in water. The solubility of welan polysaccharide in dimethyl sulfoxide and ethylene glycol has been determined by visual observation and reported only as "good" or "poor solubility" in such organic solvents (Hember & Morris, 1995). The hydration behavior of guar and xanthan gum has been studied by measuring the variation of solution viscosity with time in a rotational viscometer of samples taken from a mixing rig (To, Mitchell, Hill, Bardon, & Matthews, 1994). Here we have examined the solubility in water of LT-100 and NaHAG by means of absorption spectroscopy. The difference in %T for LT-100 and NaHAG solutions was 13.85 and 17.40, respectively. The solution with the smallest difference in %T can be considered the more soluble; then, LT-100 was 1.25 times more soluble than NaHAG. Therefore, the proposed method of preparation of NaHAG did not result in substantial reduction in solubility.

3.1.5. Rheological behavior

Fig. 6 shows the variation of G' and G'' with temperature for LT-100 and NaHAG during heating. The temperature at which $G' = G''$, i.e. $\tan\delta = 1$, is associated to a conformational transition (Nishinari, 1997; Núñez-Santiago & Tecante, 2007). Above the transition temperature, G'' was greater than G' and below this temperature, G' was greater than G'' and a continuous increase of both moduli upon cooling was observed. At the end of cooling G', was

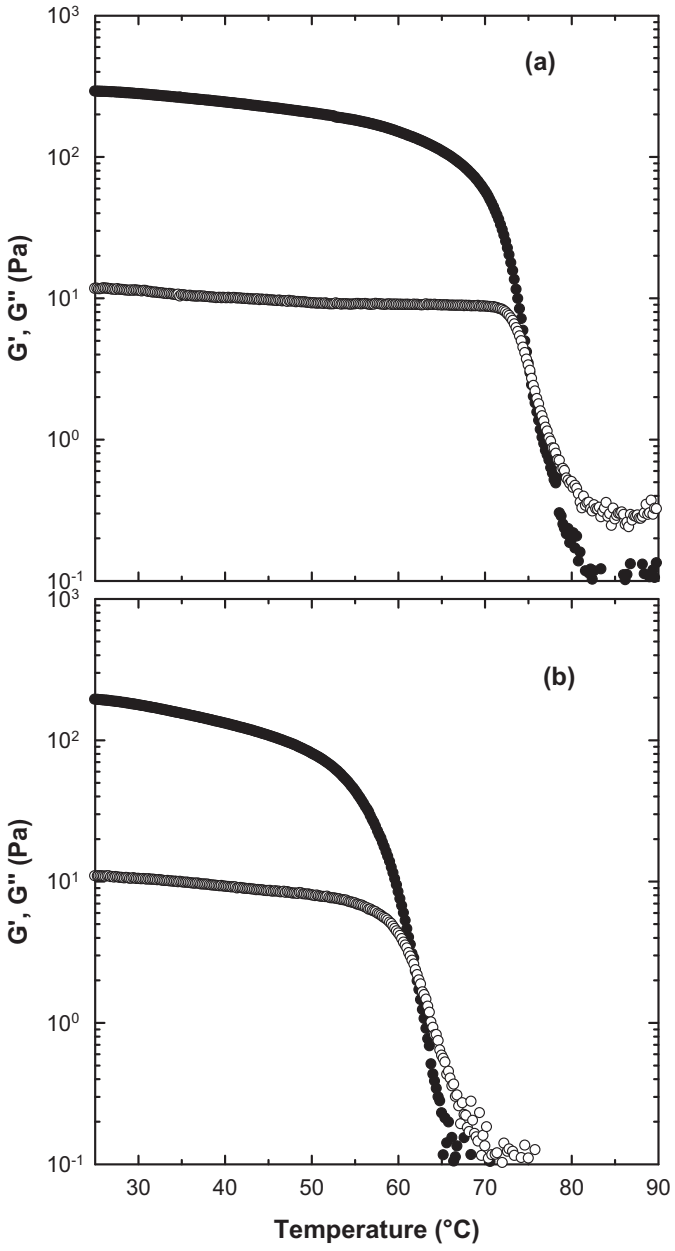

Fig. 6. Temperature dependence of G' (black symbols) and G'' (white symbols) for 1% (w/v) LT-100 (a) and NaHAG (b) on heating. T_m is given by the point at which $G' = G''$.

noticeably greater than G'' and both moduli were practically independent of temperature as a result of gelation. Table 2 shows the gel–sol transition temperatures, T_m, observed during heating, the sol–gel temperatures, T_g, determined on cooling and the thermal hysteresis, $\Delta T = T_m - T_g$, for 1% (w/v) LT-100 and NaHAG. The transition temperatures of LT-100 are significantly higher than those for NaHAG. This is due to the presence of mono and divalent cations, i.e. K^+, Na^+, Ca^{2+} and Mg^{2+}, in the commercial preparation. Specifically,

Table 2
Average T_g, T_m and ΔT (°C) for 1% (w/v) LT-100 and NaHAG.

Sample	T_m (°C)	T_g (°C)	ΔT (°C)
LT-100	75.13[a]	74.79[a]	0.346[a]
NaHAG	62.11[b]	61.30[b]	0.814[b]

Different superscript letters in the same column indicate significant difference ($p \leq 0.05$). Standard deviations for each average were lower than 0.5 °C.

the higher concentration of calcium and magnesium ions tends to increase the transition temperature of LT-100 (Huang, Singh, Tang, & Swanson, 2004). The method from which NaHAG was prepared reduced considerably the content of divalent cations and potassium ion and increased that of sodium ion. These results show the importance of counter ion content on sol–gel and gel–sol transitions. T_g and T_m of LT-100 reported in Table 2 are very close to those previously reported for this commercial preparation: 73.7 and 74.2 °C, respectively (Flores-Huicochea et al., 2013). Table 2 also shows that thermal hysteresis is negligible as ΔT is lower than 1.0 °C and is of the same order of magnitude as the standard deviation. These results are in agreement with previous observations (Flores-Huicochea et al., 2013). Huang et al. (2004) reported essentially the same transition temperature (≈70 °C), determined from the crossing over of *G*' and *G*" on cooling a 1% solution from 98 to 50 °C, for commercial LT-100 and clarified HAG (Kelcogel EX8593). Apparently, the protein content in clarified HAG was lower than in LT-100, however, it is not given in this article. Another difference is that the clarified sample was purified by ionic exchange (no further details are given) and contained a greater sodium concentration than the commercial sample. However, the ionic strengths of 1% LT-100 and EX8593 solutions without external counterions were not very different; i.e. 12 and 14 mM, respectively. The transition temperature reported by these authors is intermediate between the corresponding ones for LT-100 and NaHAG shown in Table 2. In HAG, acetyl groups located on the periphery of the double helix structure hinder helix–helix aggregation. Glyceryl groups are accommodated inside this structure and increase its thermal stability by forming additional intra and interchain hydrogen bonds. However, this changes the orientation of the adjacent carboxyl group and as a consequence the binding site for metal cations is destroyed; cation-mediated aggregation is lost, gel strength is reduced and thermal hysteresis is eliminated (Morris et al., 2012). Nevertheless, as it is unlikely that our treatment method has modified the content of acyl groups, the differences observed between both samples can be attributed to changes in ion concentration and type of ions present.

Fig. 7 shows the mechanical spectra of LT-100 and NaHAG after temperature sweeps. Both polysaccharide preparations formed gels and the variation of dynamic moduli with angular frequency is characteristic of this type of materials. The storage modulus of LT-100 gels was higher that the corresponding modulus of NaHAG gels. This can be explained on the basis of the higher content of mono and divalent cations of the commercial preparation. It is worthwhile mentioning that in a practical application, in which LT-100 is currently used, stronger and more elastic gels, i.e. gels with higher *G*' and lower tan δ, are formed. Nevertheless, it is apparent that the procedure to obtain NaHAG did not modify its ability to form gels. The behaviors depicted in Fig. 7 show that the transitions observed in rheological and DSC tests were sol–gel–sol and not only coil–helix–coil.

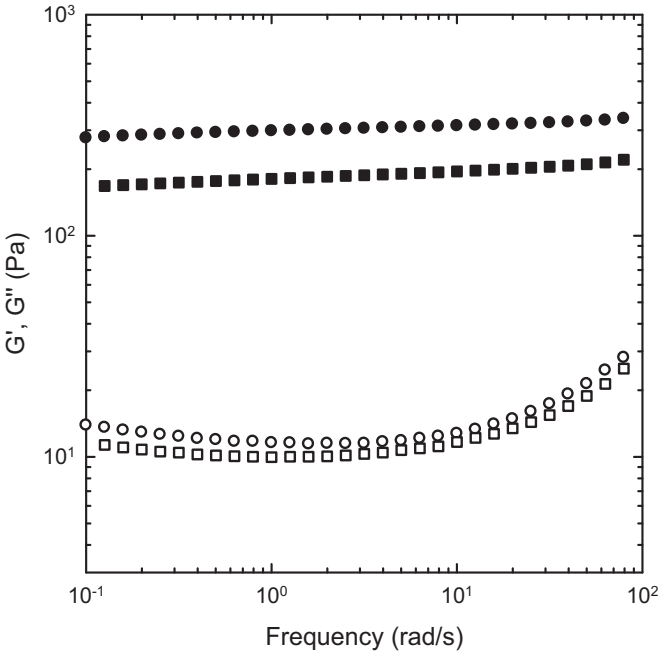

Fig. 7. Variation of *G*' (black symbols) and *G*" (white symbols) with angular frequency at 10% strain and 25 °C for 1% (w/v) LT-100 (circles) and NaHAG (squares).

3.1.6. Differential scanning calorimetry

Fig. 8 shows the thermal behavior of LT-100 and NaHAG during heating and cooling. Endothermic signals are attributed to gel–sol transitions, i.e. gel melting, and exothermic ones to sol–gel transitions, i.e. gelation. Peak temperatures were taken as gel–sol and sol–gel transitions.

The differences observed between both samples occur at least in part because divalent cations in LT-100 contribute to stabilize the structure of the polysaccharide, while in NaHAG such stabilization is given mainly by sodium ions, which are known to be less effective than calcium ions because of their low capacity to form coordinate complexes with polymer chains. The thermal transitions of high acyl gellan are broader and flatter than those for deacylated gellan (Morris, Gothard, Hember, Manning, & Robinson, 1996). As mentioned earlier, high acyl gellan has a little capacity for cation-mediated aggregation of double helices. In NaHAG the increase in the amount of sodium ions resulted in a transition temperature approximately 10 °C lower as compared with LT-100 (Table 3). The difference between melting and gelling temperatures was about 2 °C for both samples; therefore, thermal hysteresis was basically nonexistent. The broader and flatter transitions observed in our samples suggest the occurrence of different structural arrangements induced by substitution of divalent cations by sodium ions. This possibly affects helix formation, aggregation and gives rise to a more disordered structure of polysaccharide chains. Also, as acyl groups are removed from high acyl gellan, the polysaccharide regains its ability to form fibrillar networks by cation-mediated aggregation of double helices giving rise to narrower and steeper thermal transitions (Morris et al., 2012).

Table 3 shows the temperature interval over which thermal transitions took place and the associated enthalpies for LT-100 and NaHAG. Transition temperatures from rheological temperature sweeps are approximately 4.0% higher than DSC peak temperatures for both heating and cooling, but they fall within the temperature interval of DSC transitions. Therefore, both techniques produce

Table 3
Transition enthalpies (J/g) and onset, peak and offset temperatures (°C) for LT-100 and NaHAG.

Sample	Heating				Cooling			
	ΔH	T_o	T_p	T_f	ΔH	T_o	T_p	T_f
LT-100	0.11 ± 0.00[a]	64.48 ± 2.10[a]	72.40 ± 0.15[a]	76.37 ± 0.45[a]	−0.100 ± 0.01[a]	74.27 ± 0.05[a]	70.08 ± 0.24[a]	61.32 ± 0.89[a]
NaHAG	0.14 ± 0.00[b]	50.47 ± 1.66[b]	61.52 ± 0.94[b]	67.63 ± 4.42[b]	−0.072 ± 0.01[b]	67.24 ± 0.50[b]	59.22 ± 0.04[b]	47.80 ± 2.91[b]

Mean values with different letters in the same column indicate significant difference ($p \leq 0.05$).

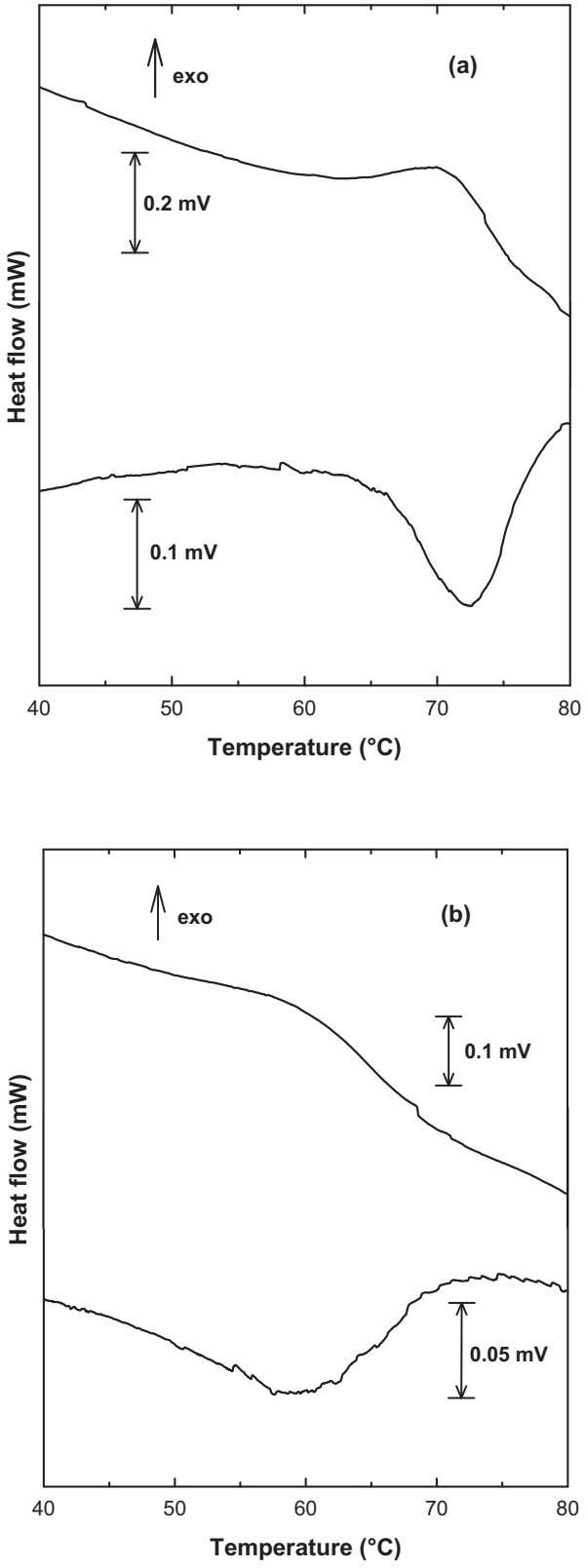

Fig. 8. DSC thermograms for 1.0% (w/v) LT-100 (a) and NaHAG (b) aqueous systems.

similar results. The transition enthalpies during heating and cooling between both preparations were significantly different. Thus, the energy required for the gel network to melt and rebuild is different for LT-100 and NaHAG. Reduction in ion content of LT-100 significantly influenced the transition temperatures and enthalpies.

4. Conclusions

The treatment method from which NaHAG was obtained did not require a water–alcohol mixture to be used as it is commonly employed to obtain polysaccharide salts, and make it easy to obtain NaHAG without intensive chemical treatment. On other hand, spectroscopic analyses of NaHAG suggest slight structure changes and a high content of sodium ions which allowed the sodium salt to be obtained. Rheological and DSC measurements show NaHAG to have significantly lower transition temperatures than LT-100 as a result of reduction in ion content. LT-100 gels exhibited slightly higher G' and lower loss angles than NaHAG gels. Thus, gels prepared from LT-100 are slightly stronger and elastic than NaHAG gels. Reduction in ion content has a greater impact on thermal transitions than on mechanical behavior in oscillatory shear. The treatment method could be used to prepare the necessary amounts of this salt for fundamental studies on the physicochemical behavior of this polysaccharide and sets the basis for extending or adapting the procedure to obtain other salt forms with other monovalent and divalent ions.

Acknowledgements

María M. Murillo-Martínez acknowledges financial support from Dirección General de Asuntos del Personal Académico-Universidad Nacional Autónoma de México (DGAPA-UNAM). The authors also acknowledge Dr. Miguel A. García-Sánchez, Professor at Universidad Autónoma Metropolitana (UAM-I) for helpful discussions.

References

Bramhachari, P. V., & Dubey, S. K. (2006). Isolation and characterization of exopolysaccharide produced by *Vibrio harveyi* strain VB23. *Letters in Applied Microbiology*, *43*, 571–577.

Coutinho, D. F., Sant, S. V., Shin, H., Oliveira, J. T., Gomes, M. E., Neves, N. M., et al. (2010). Modified gellan gum hydrogels with tunable physical and mechanical properties. *Biomaterials*, *31*, 7494–7502.

Doner, L. W. (1997). Rapid purification of commercial gellan gum to highly soluble and gellable monovalent cation salts. *Carbohydrate Polymers*, *32*, 245–247.

Doner, L. W., & Douds, D. D. (1995). Purification of commercial gellan to monovalent cation salts results in acute modification of solution and gel-forming properties. *Carbohydrate Research*, *273*, 225–233.

Flores-Huicochea, E., Rodríguez-Hernández, A. I., Espinosa-Solares, T., & Tecante, A. (2013). Sol–gel transition temperatures of high acyl gellan with monovalent and divalent cations from rheological measurements. *Food Hydrocolloids*, *31*, 299–305.

Goh, K. K. T., Haisman, D. R., & Singh, H. (2006). Characterization of a high acyl gellan polysaccharide using light scattering and rheological techniques. *Food Hydrocolloids*, *20*, 176–183.

Grasdalen, H., & Smidsrod, O. (1987). Gelation of gellan gum. *Carbohydrate Polymers*, *7*, 371–393.

Hamcerencu, M., Desbrieres, J., Khoukh, A., Popa, M., & Riess, G. (2008). Synthesis and characterization of new unsaturated esters of gellan gum. *Carbohydrate Polymers*, *71*(1), 92–100.

Hember, M. W. N., & Morris, E. R. (1995). Solubility, solution rheology and salt-induced gelation of welan polysaccharide in organic solvents. *Carbohydrate Polymers*, *27*, 23–36.

Huang, Y., Singh, P. P., Tang, J., & Swanson, B. G. (2004). Gelling temperatures of high acyl gellan as affected by monovalent and divalent cations with dynamic rheological analysis. *Carbohydrate Polymers*, *56*, 27–33.

Jansson, P. E., Lindberg, B., & Sandford, P. A. (1983). Structural studies of gellan gum, an extracellular polysaccharide elaborated by *Pseudomonas elodea*. *Carbohydrate Research*, *124*(1), 135–139.

Jay, A. J., Colquhoun, I. J., Ridout, M. J., Brownsey, G. J., Morris, V. J., Fialho, A. M., et al. (1998). Analysis of structure and function of gellans with different substitution patterns. *Carbohydrate Polymers*, *35*, 179–188.

Kačuráková, Â. M., & Wilson, R. H. (2001). Developments in mid-infrared FTIR spectroscopy of selected carbohydrates. *Carbohydrate Polymers*, *44*(4), 291–303.

Kang, K. S., Veeder, G. T., & Kaneko, T. (1982). Agar like polysaccharide produced by pseudomona species: Production and basic properties. *Applied and Environmental Microbiology*, *43*, 1086–1091.

Kuo, M.-S., Mort, A. J., & Dell, A. (1986). Identification and location of L-glycerate, an unusual acyl substituent in gellan gum. *Carbohydrate Research*, *156*, 173–187.

Matsukawa, S., Tang, Z., & Watanabe, T. (1999). Hydrogen-bonding behavior of gellan in solution during structural change observed by ^{1}H NMR and circular dichroism methods. *Progress in Colloid Polymer Science*, *114*, 15–24.
Matsukawa, S., & Watanabe, T. (2007). Gelation mechanism and network structure of mixed solution of low- and high-acyl gellan studied by dynamic viscoelasticity, CD and NMR measurements. *Food Hydrocolloids*, *21*, 1355–1361.
Mazen, F., Milas, M., & Rinaudo, M. (1999). Conformational transition of native and modified gellan. *International Journal of Biological Macromolecules*, *26*, 109–118.
Milas, M., & Rinaudo, M. (1996). The gellan sol–gel transition. *Carbohydrate Polymers*, *30*(2-3), 177–184.
Milas, M., Shi, X., & Rinaudo, M. (1990). On the physicochemical properties of gellan gum. *Biopolymers*, *30*(3-4), 451–464.
Miyoshi, E., Takaya, T., & Nishinari, K. (1996). Rheological and thermal studies of gel–sol transition in gellan gum aqueous solution. *Carbohydrate Polymers*, *30*, 109–119.
Morris, E. R., Gothard, M. G. E., Hember, M. W. N., Manning, C. E., & Robinson, G. (1996). Conformational and rheological transitions of welan, rhamsan, and acylated gellan. *Carbohydrate Polymers*, *30*, 165–175.
Morris, E. R., Nishinari, K., & Rinaudo, M. (2012). Gelation of gellan – A review. *Food Hydrocolloids*, *28*(2), 373–411.
Nakamura, K., Harada, K., & Tanaka, Y. (1993). Viscoelastic properties of aqueous gellan solutions: The effects of concentration on gelation. *Food Hydrocolloids*, *7*(5), 435–447.
Nishinari, K. (1997). Rheological and DSC study of sol–gel transition in aqueous dispersions of industrially important polymers and colloids. *Colloid Polymer Science*, *275*, 1093–1107.
Novac, O., Lisa, G., Barbu, E., Alhaique, F., & Popa, M. I. (2013). Synthesis and characterization of *N*-(2-aminoethyl)-2-acetamidyl gellan gum with potential biomedical applications. *Carbohydrate Polymers*, *98*(1), 174–177.
Núñez-Santiago, M. C., & Tecante, A. (2007). Rheological and calorimetric study of the sol–gel transition of κ-carrageenan. *Carbohydrate Polymers*, *69*(4), 763–773.
Ogawa, E., Takahashi, R., Yajima, H., & Nishinari, K. (2005). Thermally induced coil-to-helix transition of sodium gellan gum with different molar masses in aqueous salt solutions. *Biopolymers*, *79*, 207–217.
Ogawa, E., Takahashi, R., Yajima, H., & Nishinari, K. (2006). Effects of molar mass on the coil to helix transition of sodium-type gellan gums in aqueous solutions. *Food Hydrocolloids*, *20*, 378–385.
O'Neil, M. A., Selvendran, R. R., & Morris, V. J. (1983). Structure of the acidic extracellular gelling polysaccharide produced by *Pseudomonas elodea*. *Carbohydrate Research*, *124*, 123–133.
Prajapati, V. D., Jani, G. K., Zala, B. S., & Khutliwala, T. A. (2013). An insight into the emerging exopolysaccharide gellan gum as a novel polymer. *Carbohydrate Polymers*, *93*, 670–678.
Rodríguez-Hernandez, A. I., Durand, S., Garnier, C., Tecante, A., & Doublier, J. L. (2003). Rheology-structure properties of gellan systems: Evidence of network formation at low gellan concentrations. *Food Hydrocolloids*, *17*, 621–628.
Sanderson, G. R., & Clark, R. C. (1984). Gellan gum, a new gelling polysaccharide. In G. O. Phillips, D. J. Wedlock, & P. A. Williams (Eds.), *Gums and stabilizers for the food industry* (pp. 201–210). Oxford: Pergamon Press.
Sartori, C., Finch, D. S., Ralph, B., & Gilding, K. (1997). Determination of the cation content of alginate thin films by FTIR spectroscopy. *Polymer*, *38*(1), 43–51.
To, K.-M., Mitchell, J. R., Hill, S. E., Bardon, L. A., & Matthews, P. (1994). Measurement of hydration of polysaccharides. *Food Hydrocolloids*, *8*, 243–249.
Upstill, C., Atkins, E. D. T., & Attwool, P. T. (1986). Helical conformation of gellan gum. *International Journal of Biological Macromolecules*, *8*, 275–288.